

LETTERS

Disruption of extended defects in solid oxide fuel cell anodes for methane oxidation

Juan Carlos Ruiz-Morales^{1,†}, Jesús Canales-Vázquez^{1,†}, Cristian Savaniu¹, David Marrero-López², Wuzong Zhou³ & John T. S. Irvine¹

Point defects largely govern the electrochemical properties of oxides: at low defect concentrations, conductivity increases with concentration; however, at higher concentrations, defect-defect interactions start to dominate^{1,2}. Thus, in searching for electrochemically active materials for fuel cell anodes, high defect concentration is generally avoided. Here we describe an oxide anode formed from lanthanum-substituted strontium titanate (La-SrTiO₃) in which we control the oxygen stoichiometry in order to break down the extended defect intergrowth regions and create phases with considerable disordered oxygen defects. We substitute Ti in these phases with Ga and Mn to induce redox activity and allow more flexible coordination. The material demonstrates impressive fuel cell performance using wet hydrogen at 950 °C. It is also important for fuel cell technology to achieve efficient electrode operation with different hydrocarbon fuels^{3,4}, although such fuels are more demanding than pure hydrogen. The best anode materials to date—Ni-YSZ (yttria-stabilized zirconia) cermet⁵—suffer some disadvantages related to low tolerance to sulphur⁶, carbon build-up when using hydrocarbon fuels⁷ (though device modifications and lower temperature operation can avoid this^{8,9}) and volume instability on redox cycling. Our anode material is very active for methane oxidation at high temperatures, with open circuit voltages in excess of 1.2 V. The materials design concept that we use here could lead to devices that enable more-efficient energy extraction from fossil fuels and carbon-neutral fuels.

Over the past few years there has been a growing interest in perovskite-based materials in the search for alternative materials to Ni-YSZ cermets as fuel electrodes in solid oxide fuel cells (SOFCs)¹⁰. Such perovskites are normally oxygen stoichiometric or substoichiometric: here we seek to explore perovskites that are nominally oxygen overstoichiometric as SOFC fuel electrodes. Initially we focus on phases with extended oxygen-rich defects, and then attempt to destabilize these extended defects by reducing the degree of oxygen excess. Titanates with nominal oxygen overstoichiometry are especially interesting owing to their very high electronic conductivity, stability in reducing conditions and resistance to sulphur poisoning^{11–14}. Oxides belonging to the La_{1-x}Sr_xTiO_{3-δ} system have been previously studied as anode materials showing moderate performance compared to those of the state of the art materials, but better catalytic properties and ionic conductivity are desirable^{15,12}.

The performance of titanate-based materials was greatly improved by using composites with CeO₂ (ref. 15), based on the catalytic properties of the ceria. These lanthanum strontium titanates are usually treated in the literature as simple cubic perovskites, although the presence of extra oxygen beyond the ABO₃ stoichiometry plays a

critical role in both the structure and the electrochemical properties, as summarized in Fig. 1. The lower members of the La_{1-x}(Ti_{1-x}O_{3-δ})_{n+2} series, $n < 7$, are layered phases, having oxygen-rich planes in the form of crystallographic shears joining consecutive

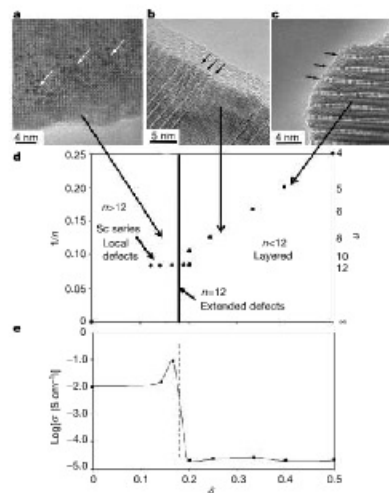


Figure 1 | Relation between microstructure, composition and conductivity of the La_{0.9}Sr_{0.1}Ti_{1-x}O_{3-δ} series. **a–c**, HRTEM images of samples varying from disordered extended defects (**a**, $n = 12$) through random layers of extended defects (**b**, $n = 8$) to ordered extended planar oxygen excess defects (**c**, $n = 5$). **d**, The location of these phases on the composition map, with $1/n$ plotted against oxygen excess δ in perovskite unit ABO_{3-δ}. **e**, Defect electronic conductivity of grain component as determined by a.c. impedance spectroscopy on samples quenched from 1,300 °C in air, also plotted against δ . 'Sc series' refers to samples in series (La_{0.9}Sr_{0.1})_{n+2}(Ti_{1-x})_{n+2}O_{3n+2-2x} (ref. 14).

Table 1 | Properties of La_{0.9}Sr_{0.1}Ti_{1-x}O_{3-δ} electrodes

Electrode	R_p ($\Omega \text{ cm}^2$)		OCV (V)	Representative electrode grain size (μm)
	97.7% H ₂ /2.3% H ₂ O	97.7% CH ₄ /2.3% H ₂ O		
La _{0.9} Sr _{0.1} O _{3-x} , $x = 0^*$	2.97	8.93	0.98	1
M = Sc, ($x = 0.6$) [†]	0.50	1.20	1.30	0.5–1.0
M = Mn ($x = 1$)	0.43	1.14	0.98	0.8
Mn ($x = 0.5$), Ga ($x = 0.5$)	0.20	0.57	1.25	0.8

Comparison of open circuit voltage (OCV) and polarization resistance (R_p) measured in indicated gas compositions at 900 °C on oxidized and undoped La_{0.9}Sr_{0.1}Ti_{1-x}O_{3-δ}. ^{*}Ref. 9; (ref. 14); (ref. 25).

blocks. These planes become more sporadic with increasing n (that is, decreasing the oxygen content) until they are no longer crystallographic features, rendering local oxygen-rich defects randomly distributed within a perovskite framework, $n > 11$ (ref. 16). Substitution of Ti⁴⁺ by Nb⁵⁺ or Sc³⁺ demonstrates that the oxygen excess parameter (δ) critically determines whether defects are ordered or disordered, with $\delta = 0.167$ being a critical parameter. The presence of such disordered defects appears to strongly affect the redox characteristics of the oxide, as indicated by marked effects on conductivity induced by mild reduction (Fig. 1). Although the materials from this lanthanum strontium titanate oxygen excess series are much easier to reduce, and hence exhibit much higher electronic conductivity than their oxygen stoichiometric analogues, they do not exhibit electrochemical performance comparable to such an effective oxide anode as La_{0.75}Sr_{0.25}Co_{0.25}Mn_{0.75}O_{3-δ} (ref. 10). This we attribute to the inflexibility of the co-ordination demands of titanium, which strongly prefers octahedral coordination in the perovskite environment.

In order to make the B-site co-ordination more flexible and hence to improve electrocatalytic performance, we have introduced various dopants to replace Ti in La_{0.9}Sr_{0.1}Ti_{1-x}O_{3-δ}-based fuel electrodes, Table 1, and found the most successful to be a combination of Mn and the trivalent Ga ion. Mn supports p-type conduction in oxidizing conditions, and has been previously shown to promote electroreduction under SOFC conditions^{13,14}. Furthermore, Mn is known to accept lower coordination numbers in perovskites¹⁷,

especially for Mn³⁺, and thus it may facilitate oxide-ion migration. Similarly Ga is well known to adopt lower co-ordination than octahedral in perovskite-related oxides. The possibility of mixed ionic/electronic conduction is very important, because it would allow the electro-oxidation process to move away from the three-phase electrode/electrolyte/gas interface onto the anode surface, with considerable catalytic enhancement¹⁸.

La_{0.9}Sr_{0.1}Ti_{1-x}Mn_{0.5}Ga_{0.5}O_{3-δ} (LSTMG) powders were prepared by solid state reaction from stoichiometric amounts of high purity La₂O₃, SrCO₃, TiO₂, Mn₂O₃ and Ga₂O₃ fired for 24–48 h. Polarization measurements were performed in a three-electrode arrangement. The electrolyte was a sintered 8 mol% Y₂O₃ stabilized ZrO₂ (YSZ) pellet of 2 mm thickness and 20 mm diameter. La_{0.9}Sr_{0.1}MnO₃ (LSM) and Pt were used as counter-electrode and reference electrode, respectively. The anode was prepared in two configurations, first as a 60- μm -thick layer of 50:50 LSTMG:YSZ and second as an optimized anode with four layers, with graded concentration of YSZ. Each layer was pre-fired at 300 °C and all of them co-fired at 1,200 °C for 2 h. Electrical contacts to the anodes were formed using an Au mesh with small amounts of Au paste to ensure contacting and to avoid any additional catalytic effect. Fuel-cell performance was obtained for these materials as SOFC anodes with 330- μm -thick YSZ/Al₂O₃ electrolyte and LSM cathode. Platinum paste coated onto LSM and fired at 900 °C was used as the cathode current collector.

La_{0.9}Sr_{0.1}Ti_{1-x}Mn_{0.5}Ga_{0.5}O_{3-δ} forms as a single-phase perovskite on firing at 1,400 °C. The structure obtained can be refined as monoclinic, with $a = 5.5287(9)$ Å, $b = 7.8098(5)$ Å, $c = 5.3096(6)$ Å, $\beta = 92.295(7)^\circ$, $V = 229.08(6)$ Å³. No chemical reactions were observed by X-ray diffraction on firing an intimate mixture of LSTMG and YSZ pressed powder at 1,200 °C in air for 80 h, indicating good chemical compatibility. The phase is stable under fuel conditions at 1,000 °C; the perovskite structure is retained on

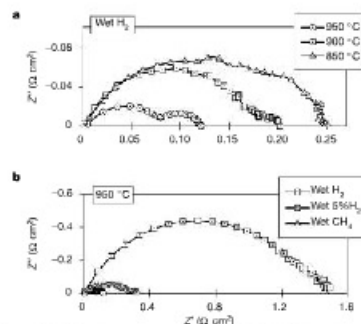


Figure 2 | Polarization measurements on LSTMG/YSZ with varying temperatures and atmospheres. Polarization impedances were measured **a**, under humidified hydrogen at different temperatures, and **b**, under different atmospheres at 950 °C, all humidified at 20 °C on a screen-printed graded La_{0.9}Sr_{0.1}Mn_{0.5}Ga_{0.5}O_{3-δ}/YSZ working electrode on a 2 mm YSZ electrolyte with La_{0.9}Sr_{0.1}MnO₃/Pt counter and reference electrodes. Z' and Z'' are respectively the real and the imaginary parts of the complex impedance.

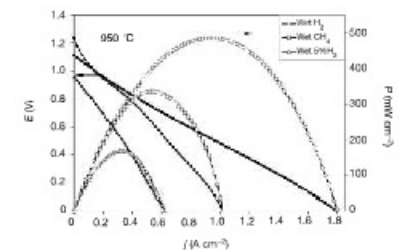


Figure 3 | Performance plots in different atmospheres. Fuel cell performance plots for different fuel gas compositions each containing 2.3% of water at a four-layer optimized LSTMG anode (circle: pure H₂; square: pure CH₄; triangle: 5% H₂) on a 330- μm -thick YSZ electrolyte, with LSM cathode in unhumidified oxygen. E is potential difference between electrodes, j is current density and P is power density.

¹School of Chemistry, University of St Andrews, St Andrews, Fife KY16 9ST, UK; ²Department of Inorganic Chemistry, University of La Laguna, 38200, Canary Islands, Spain; ³Present address: Department of Inorganic Chemistry, University of La Laguna, 38200, Canary Islands, Spain; (†C.R.-M.); Instituto de Ciencia de los Materiales ICMA-B-CSC, 08993, Barcelona, Spain (†C.-V.).

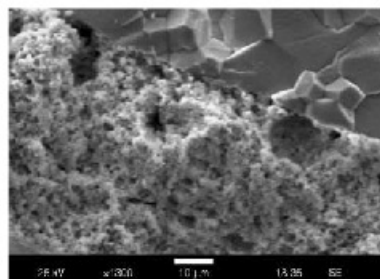


Figure 4 | Electrode interface. Scanning electron microscope image, showing the cross-section of a fuel cell after testing.

firing in 4.9% H_2 /2.3% H_2O /92.8% Ar (thereafter termed wet 5% H_2) for 24 h, with the cell changing to orthorhombic $a = 5.5343(6) \text{ \AA}$, $b = 7.8239(4) \text{ \AA}$, $c = 5.5322(7) \text{ \AA}$, $V = 239.54(6) \text{ \AA}^3$. Detailed high-resolution transmission electron microscopy (HRTEM) studies show exactly the same features that were observed for $La_2Sr_2Ti_2O_{10}$ ($n = 12$), that is, this phase is within the localized defect region, as predicted in Fig. 1 for $\delta < 0.167$. On re-oxidation of LSTMG in air, in a thermogravimetric analyser, a weight increase of 0.37% was observed in a step between 400 and 600 °C, corresponding to a change in oxygen content of about 0.5 oxygen atoms per formula unit, consistent with Mn^{3+} to Mn^{4+} reoxidation. Some further weight gain of about 0.07% (0.1 O) was observed on holding at 900 °C which may be related to Ti^{3+} to Ti^{4+} reoxidation and is fairly typical for these titanates¹¹.

The total conductivity is 0.0045 Scm^{-1} in air at 900 °C and increases up to 0.5 Scm^{-1} at 10^{-15} atm. Activation energies for conduction are 0.16 eV for 200–700 °C, and 0.56 eV for 700–900 °C in wet 5% H_2 . The conductivity of $La_2Sr_2Ti_2Mn_{0.5}Ga_{0.5}O_{10}$ was also measured as a function of oxygen partial pressure at 800 °C and 900 °C. The material shows typical n-type conductivity as the dominant conduction mechanism, but some evidence of p-type conductivity can be found at $p_{O_2} > 0.5$ atm.

The anode polarization resistance was measured using three-electrode geometry as previously described¹¹. Results at different temperatures in humidified hydrogen are shown in Fig. 2a and in different atmospheres at 950 °C in Fig. 2b using an optimized anode made of four graded layers with varying LSTMG:YSZ ratios and total thickness 140 μm . The polarization resistances in wet H_2 (97.7% H_2 , 2.3% H_2O) were $0.12 \Omega \text{ cm}^2$ at 950 °C, $0.20 \Omega \text{ cm}^2$ at 900 °C and $0.25 \Omega \text{ cm}^2$ at 850 °C. The polarization resistances were $0.12 \Omega \text{ cm}^2$ in wet H_2 , 1.5 $\Omega \text{ cm}^2$ in wet 5% H_2 and a remarkably low value, $0.36 \Omega \text{ cm}^2$, in wet CH_4 (97.7% CH_4 , 2.3% H_2O), at 950 °C. These polarization resistances were attained after about 24 h in fuel conditions; initial polarization resistances were 2–3 times higher. This long time period to achieve equilibration is fairly typical for donor doped strontium titanates that are not cation vacancy compensated, and we attribute this to reorganization of a complex defect structure. The best previous results using metal-free oxide anodes only achieved polarization resistances of twice these values and with much lower OCVs (open circuit voltages) in methane⁹. These polarization resistances are about 15 times less than previously achieved without Mn/Ga addition¹¹, and less than 50% of the values obtained using just Mn, all for electrodes with similar microstructures (Table 1). Furthermore, these results are comparable with the best cermet electrode performances, and allow both operation in low steam hydrocarbon fuels and good mechanical redox stability.

570

The OCVs matched the value predicted by the Nernst equation, 0.97 V and 1.13 V at 950 °C, for wet 5% H_2 and wet H_2 , respectively. The OCVs in wet CH_4 , for a single layer 50:50 YSZ:LSTMG anode, were: 1.39 V at 950 °C, 1.32 V at 900 °C and 1.36 V at 850 °C. These values were reproducible after two days of testing in wet 5% H_2 , wet H_2 and wet CH_4 . For a four-layer anode, in wet CH_4 , the OCVs were: 1.23 V, 1.17 V and 1.16 V at 950 °C, 900 °C and 850 °C, respectively. The high OCVs compared to those typically observed with methane fuels are more significant than, but broadly similar to, that for the addition of precious metal to copper ceria anodes²⁰. It seems clear that the thicker, more complex anode structure is less able to fully activate methane at the electrode/electrolyte interface, even though the electrochemical performance of the complex anode is superior in terms of polarization resistance. The OCV trend observed at the thicker electrode is similar to that obtained by Liu and Barnett²¹ which they initially attributed to partial oxidation of produced carbon, but later²² suggested was due to the oxidation of hydrogen, produced by methane reforming with the humidified methane reaching equilibrium at the anode. Here the high OCV we obtained at the thin electrode (1.4 V) implies full oxidation of equilibrated wet CH_4 , as this potential is the expected OCV in such an atmosphere.

Figure 3 shows the performance of the LSTMG anode in different atmospheres, at 950 °C, using a two-electrode set-up. The maximum power density in wet H_2 was close to 0.5 W cm^{-2} and the power density in wet CH_4 is two times higher than in 5% H_2 , reaching a value of about 0.35 W cm^{-2} . The different slopes in the current-voltage plots under methane seem to suggest different reactions. After running a fuel cell for two days, cycling from 950 °C to 850 °C, in wet 5% H_2 , wet H_2 and wet methane, no traces of carbon could be detected visually or by thermal analysis. This anode exhibited a very fine microstructure, Fig. 4, with uniform particle size just less than 1 μm , an estimated 45% porosity and a clean interface with the electrolyte.

This work has demonstrated the concept of inducing functionality through disorder of extended defects. Through partially replacing titanium with some manganese and gallium, an SOFC anode with similar performance in hydrogen to nickel/zirconia cermets has been achieved. In contrast with these cermets, the electrode is remarkably active for the oxidation of CH_4 at high temperatures in the absence of excess steam; moreover, high OCVs reaching stable values between 1.2 V and 1.4 V have been obtained. Optimization of the microstructure allows a very marked improvement in the properties of the anode, but there remains a problem with fairly low lateral conductivity, which (especially for SOFC designs with long current paths) will require an additional current collector for practical application. Thus this material shows considerable promise as an electrochemical anode yielding the lowest polarization results so far reported for an oxide anode and excellent prospects for direct hydrocarbon use.

Received 16 September; accepted 1 November 2005.

- Kilner, J. A. & Steele, B. C. H. The effect of ion size on the energy of association between oxygen vacancies and dopant cations in oxide solid electrolytes. *J. Electrochem. Soc.* **129**, C143–C148 (1982).
- Irvine, J. T. S., Feighery, A. J., Fagg, D. P. & Garcia-Martin, S. Structural studies on the optimization of fast oxide ion transport. *Solid State Ionics* **136/137**, B79–B85 (2000).
- Ahlsson, A. et al. Advanced anodes for high-temperature fuel cells. *Nature Mater.* **3**, 17–27 (2004).
- Prinzl, S., Hansen, J. R., Grahl-Madsen, L. & Larsen, P. H. Sn-doped La_2O_3 anode for solid oxide fuel cells. *J. Electrochem. Soc.* **148**, A74–A81 (2001).
- Singhal, S. C. & Kendall, K. *High Temperature Solid Oxide Fuel Cells: Fundamentals, Design and Applications* (Elsevier, Oxford, 2004).
- Mitsuzaki, Y. & Yasuda, I. The poisoning effect of sulfur-containing impurity gas on a SOFC anode: Part I. Dependence on temperature, time and impurity concentration. *Solid State Ionics* **132**, 261–269 (2000).
- Zhu, W. Z. & Devi, S. C. A review on the status of anode materials for solid oxide fuel cells. *Mater. Sci. Eng. A* **362**, 228–239 (2003).
- Park, S., Vohs, J. M. & Gorte, R. J. Direct oxidation of hydrocarbons in a solid-oxide fuel cell. *Nature* **404**, 265–267 (2000).

- Perry, E., Tsai, T. & Barnett, S. A. A direct-methane fuel cell with a ceria-based anode. *Nature* **400**, 649–651 (1999).
- Tao, S. W. & Irvine, J. T. S. A redox-stable efficient anode for solid-oxide fuel cells. *Nature Mater.* **2**, 320–323 (2003).
- Canales-Vázquez, J., Tao, S. W. & Irvine, J. T. S. Electrical properties in $La_2Sr_2Ti_2O_{10}$ a potential anode for high temperature fuel cells. *Solid State Ionics* **159**, 159–165 (2003).
- Morina, O. A., Carfield, N. L. & Stevenson, J. W. Thermal, electrical, and electrochemical properties of lanthanum-doped strontium titanate. *Solid State Ionics* **149**, 21–28 (2002).
- Mukundan, R., Brosha, E. L. & Garzon, F. H. Sulfur tolerant anodes for SOFCs. *Electrochem. Solid-State Lett.* **7**, A4–A7 (2004).
- Canales-Vázquez, J., Ruiz-Morales, J. C., Irvine, J. T. S. & Zhou, W. Sr-substituted oxygen excess titanates as fuel electrodes for SOFC. *J. Electrochem. Soc.* **152**, 1458–1465 (2005).
- Morina, O. A. & Pedersen, L. R. in *Proc. 5th European Solid Oxide Fuel Cell Forum* (ed. Huijssmans, J.) 481–489 (European Fuel Cell Forum, Oberrohrdorf, Switzerland, 2002).
- Canales-Vázquez, J., Smith, M. J., Irvine, J. T. S. & Zhou, W. Studies on the reorganization of extended defects with increasing n in the perovskite-based $La_{2-x}Ti_xO_{3-\delta}$ series. *Adv. Funct. Mater.* **15**, 1000–1008 (2005).
- Hollappel, P., Bradley, J. L., Irvine, J. T. S., Kaiser, A. & Mogensen, M. Electrochemical characterization of ceramic SOFC anodes. *J. Electrochem. Soc.* **148**, A923–A929 (2001).

- Irvine, J. T. S. et al. Optimisation of perovskite titanates and niobates as anode materials for SOFCs. in *Proc. 4th European SOFC Forum* (ed. McEvoy, A. J.) 471–477 (European Fuel Cell Forum, Oberrohrdorf, Switzerland, 2000).
- Pospelmeier, K. R., Lennartz, M. E. & Longo, J. M. $CaMnO_3$ and Ca_2MnO_7 — new oxygen-defect perovskite-type oxides. *J. Solid State Chem.* **44**, 89–96 (1982).
- McIntosh, S., Vohs, J. M. & Gorte, R. J. Effect of precious-metal dopants on SOFC anodes for direct utilization of hydrocarbons. *Electrochem. Solid-State Lett.* **6**, A240–A243 (2003).
- Liu, J. & Barnett, S. A. Operation of anode-supported solid oxide fuel cells on methane and natural gas. *Solid State Ionics* **158**, 11–16 (2003).
- Lin, Y., Zhan, Z., Liu, J. & Barnett, S. A. Direct operation of solid oxide fuel cell with methane fuel. *Solid State Ionics* **176**, 1827–1835 (2005).
- Ovile, A., Ruiz-Morales, J. C., Canales-Vázquez, J., Morero-López, D. & Irvine, J. T. S. Mn-substituted titanates as efficient anodes for direct methane SOFCs. *Solid State Ionics* (submitted).

Acknowledgements This work was funded partly by a EU Marie Curie Fellowship and by EPSRC.

Author Information Reprints and permissions information is available at <http://www.nature.com/reprintsandpermissions>. The authors declare no competing financial interests. Correspondence and requests for materials should be addressed to J.T.S. (jts@slc-andc.uk).

571